Generation of long-range correlations in large systems as an optimization problem

Hossein Hamzehpour[1] and Muhammad Sahimi[2,*]
[1]*Institute for Advanced Studies in Basic Sciences, Gava Zang, Zanjan 45195-1159, Iran*
[2]*Mork Family of Department of Chemical Engineering and Materials Science, University of Southern California, Los Angeles, California 90089-1211, USA*
(Received 2 January 2006; published 22 May 2006)

We propose an efficient method of generating long-range correlations in large systems. The development of this method was motivated by the problem of constructing an optimal model for a large-scale porous medium. There are typically long-range correlations in the properties of such porous media, such as their permeability and porosity, for which there are usually only limited data. The optimal model must not only honor (preserve) the available data and their correlation function, but also accurately predict the *future* behavior of fluid flow in the media. We formulate the problem of generating the long-range correlations as one of optimization, and utilize simulated annealing to generate a d-dimensional array which contains the correlations and honors the existing data. The optimization process is based on the data's correlation function. The method is, therefore, free of the many numerical difficulties and/or limitations that most previous techniques suffer from. It is completely general and may be used for generating long-range correlations with *any* type of correlation function, in *both* isotropic and anisotropic media. Representative examples are presented, and the method's efficiency and accuracy are discussed.

DOI: 10.1103/PhysRevE.73.056121 PACS number(s): 05.90.+m, 47.56.+r, 05.40.−a

I. INTRODUCTION

Long-range correlations are ubiquitous in nature. Examples include the correlations that exist in the porosity, permeability [1–3], and elastic constants of, and wave speeds [4] in, field-scale porous media, the distribution of fluid velocities in turbulent flow [5], and in the human heartbeat rates [6,7]. In many cases, such correlations are characterized by power-law correlation functions and follow the statistics of the fractional Brownian motion (FBM) $B(\mathbf{r})$, for which the two-point correlation function $C(r)$ is given by

$$C(r) = C_1 r^{2H}, \tag{1}$$

where $C_1 = C(r=1)$. Here, H is the Hurst exponent that characterizes the type of correlations. For $H > 1/2$ ($H < 1/2$) one has persistent or positive (antipersistent or negative) correlations in the successive increments of the FBM, while for $H = 1/2$ the trace of an FBM follows Brownian motion and, thus, the increments are uncorrelated. Figure 1 presents samples of one-dimensional (1D) FBM arrays for two values of the Hurst exponent H, which exhibit the typical patterns seen in 1D FBM arrays for H both above and below 0.5. While the Hurst exponent is positive, one may view Eq. (1) more generally and allow H to represent a parameter than can take on both positive and negative values. Another important property of a FBM is that its successive increments follow a Gaussian distribution (albeit with long-range correlations).

Modeling of correlated systems with power-law correlation functions entails accurate and efficient generation of the correlations in the models. Accuracy is important in the sense that the correlations must be preserved in every part of the system and not in, for example, a part of it. Efficiency is crucial because the size of the systems to be modeled is often very large. For example, the geological models that represent the distribution of the porosities and permeabilities of oil reservoirs are typically represented by a three-dimensional (3D) computational grid with a few million grid points or blocks. In addition, due to the stochastic nature of such systems, one must generate several realizations of them and average the properties of interest over all the realizations. Therefore one must generate many large 3D correlated arrays that are characterized by Eq. (1) or other types of correlation functions.

Several methods have been suggested in the past for generating long-range correlations with power-law correlation functions. A convenient representation of such correlations is through their spectral density $S(\boldsymbol{\omega})$, the Fourier transform of their covariance. For a d-dimensional FBM for which the correlation function is given by Eq. (1), one has

$$S(\boldsymbol{\omega}) = \frac{a(d)}{\left(\sum_{i=1}^{d} \omega_i^2\right)^{H+d/2}}, \tag{2}$$

where $\boldsymbol{\omega} = (\omega_1, \ldots, \omega_d)$, and $a(d)$ is a d-dependent constant. Equation (2) provides a method for generating a FBM array with correlated numbers that follow the correlation function given by Eq. (1), using a fast Fourier transformation (FFT) technique. In this method, one first generates random numbers, uniformly distributed in [0,1), and assigns them to the sites of a d-dimensional lattice. The FT of the resulting d-dimensional array is then computed numerically and the results are multiplied (filtered) by $\sqrt{S(\boldsymbol{\omega})}$. The inverse FT of the results represents an array of correlated numbers with a correlation function given by Eq. (1). To avoid the problem associated with the periodicity of the array arising as a result of using FT one must generate an array with a size much

*Corresponding author. Electronic address: moe@iran.usc.edu

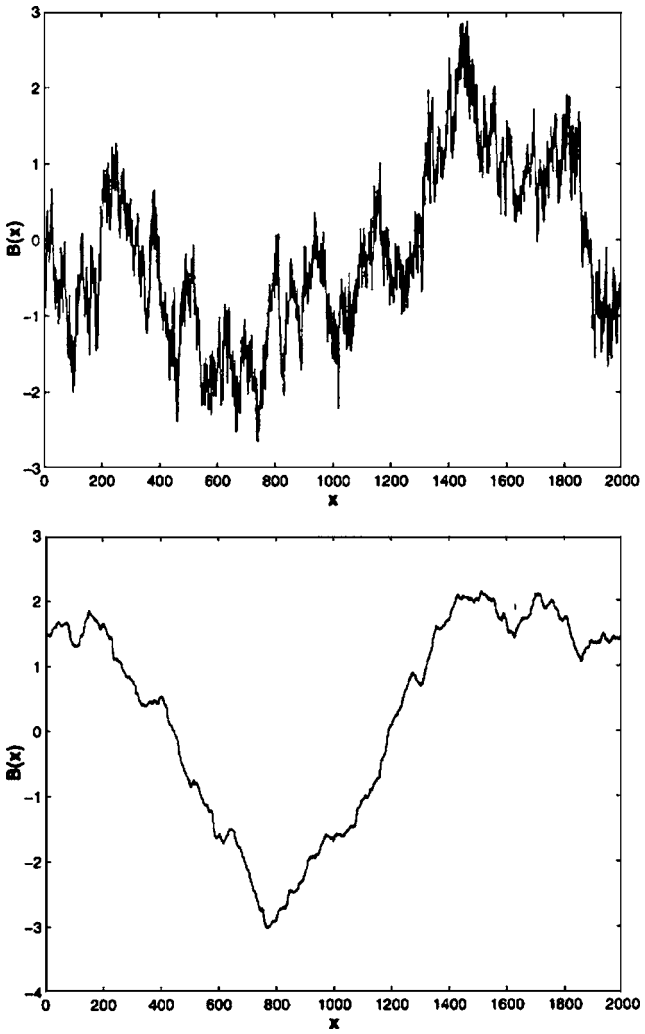

FIG. 1. One-dimensional FBM arrays for $H=0.3$ (top) and $H=0.8$ (bottom).

larger than the actual size to be used in the simulation of a physical system and use its central part. This reduces greatly the efficiency of the FFT method and limits its use to relatively small systems [8,9].

Makse *et al.* [8] and Pang *et al.* [10] modified the FFT method for better accuracy and efficiency. Since the correlation function (1) has a singularity at $r=0$, they considered a slightly different correlation function,

$$C(\mathbf{r}) = \left(1 + \sum_{i=1}^{d} r_i^2\right)^{-\gamma/2}, \tag{3}$$

which, in the limit $r \to \infty$, has the same qualitative behavior as Eq. (1). The FT of the correlation function given by Eq. (3) can be determined analytically, and is given by

$$S(\boldsymbol{\omega}) = \frac{2\pi^{d/2}}{\Gamma(\beta+1)}\left(\frac{\omega}{2}\right)^{\beta} K_{\beta}(\omega). \tag{4}$$

Here, $\beta=\frac{1}{2}(\gamma-d)$, $\omega=|\boldsymbol{\omega}|$, K_β is the modified Bessel function of order β, and Γ is the gamma function. For $\omega \ll 1$, one has the asymptotic relation that $K_\beta(\omega) \sim \omega^{\beta}$. The correlated array

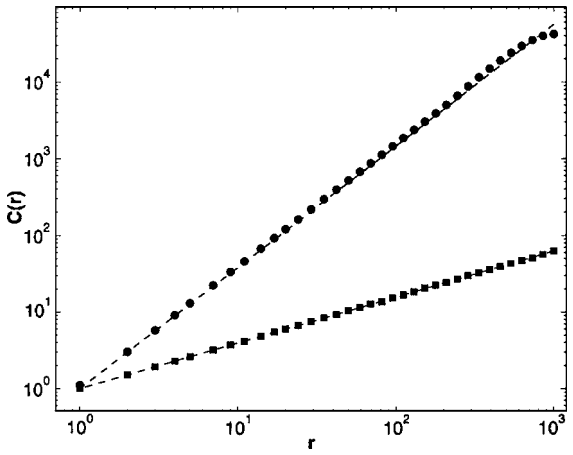

FIG. 2. The correlation functions for 1D FBM arrays of size $n=2000$, shown in Fig. 1, with $H=0.3$ (squares) and $H=0.8$ (○). Dashed lines show the fit of the data.

generated based on Eqs. (3) and (4) corresponds to a FBM with the Hurst exponent, $H=1-\frac{1}{2}\gamma$.

Voss [11] suggested another technique for generation of the FBM arrays, which is usually referred to as the successive random addition (SRA) method. In 1D one starts with the two end points in the interval [0,1], and assigns a zero value to them. Gaussian random numbers Δ_0 are then added to these values. Next, new points are added at a fraction r of the previous stage by linearly interpolating between the old points, and adding Gaussian random numbers Δ_1 to the new points. Thus, given a sample of N_i points at stage i with resolution λ, stage $i+1$ with resolution $r\lambda$ is generated by first interpolating $N_{i+1}=(N_i-1)(1/r-1)$ new points from the old ones, and then adding Gaussian random numbers Δ_i to all of the new points. At stage i with $r<1$, the Gaussian random numbers have a variance, $\sigma_i^2 \sim r^{2iH}$, consistent with the FBM. For example, with $r=1/3$ and $N_i=5$, the old (o) and new (n) points are in the order (onnonnonnonno), so that there are $N_{i+1}=8$ new points in the array. The process is continued until the desired length of the data array is reached. The method can easily be extended to any dimension. It is not, however, very efficient if large 3D correlated arrays are to be generated. In addition, extending the method for generating *anisotropic* 2D or 3D arrays is difficult (see below).

One may also utilize the Weierstrass-Mandelbrot function [9,11,12] to generate FBM arrays. In this method one first divides the interval [0,1] into $n-1$ equally spaced subintervals, where n is the size of the array to be generated, and assigns zero value to all the points in the interval. Then, to point i at a distance x_i from the origin one adds a random number generated by the Weierstrass-Mandelbrot function $W(x)$ defined by

$$W(x_i) = \sum_{j=-\infty}^{\infty} C_j r^{jH} \sin(2\pi r^{-j} x_i + \phi_j), \tag{5}$$

where C_j and ϕ_j are random numbers distributed according to Gaussian and uniform distributions, respectively, and r is a measure of the gaps between the frequencies, which is usu-

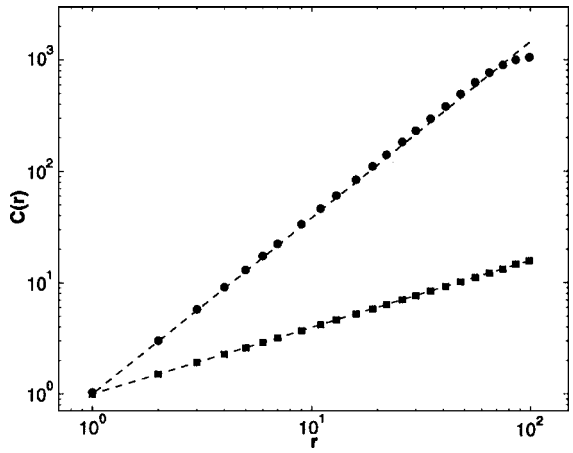

FIG. 3. The correlation functions for 2D FBMs of size $n=200\times200$ with $H=0.3$ (squares) and $H=0.8$ (○). Dashed lines show the fit of the data.

ally chosen to be small so that the gaps are also small. The variance of C_j is proportional to r^{2jH}, and the random phases ϕ_j are distributed uniformly on $[0,2\pi]$. Usually, the infinite series in Eq. (5) is approximated by a finite one but with a large number of terms (typically, $-70\leqslant j\leqslant 70$) to ensure its accuracy. Although the power spectrum of the resulting array is discrete and does not contain all the frequencies, its spectral density (in 1D) is still proportional to $\omega^{-(2H+1)}$, in agreement with Eq. (2). This method is not efficient at all in 2D or 3D [12]. It is also not clear how to extend it to anisotropic systems.

In this paper, we propose an efficient method for generation of large d-dimensional arrays with long-range correlations. The method is applicable to *any* type of correlation function, although the numerical results that are presented in this paper are for those for which Eq. (1) holds. It can be used for generating long-range correlations in both isotropic and anisotropic systems. As explained below, one main advantage of the method is that, not only can it generate long-range correlations in *both* isotropic and anisotropic systems, but can also preserve the observed data for parts of the same systems (see below). None of the previous methods can preserve the observed data. Although kriging methods [13] can also preserve the observed data and generate d-dimensional arrays with a given correlation function, they are *deterministic* techniques which can generate only a *single* realization of a system for which limited data are available and the structure of the correlation function is known. As mentioned above, in practice one often needs to generate many realizations of the same system.

The plan of this paper is as follows. In the next section we describe the method. Section III presents the results and discusses the efficiency and accuracy of the method.

II. GENERATION OF LONG-RANGE CORRELATIONS AS AN OPTIMIZATION PROBLEM

The method was motivated by an important physical problem, namely, modeling of large-scale porous media,

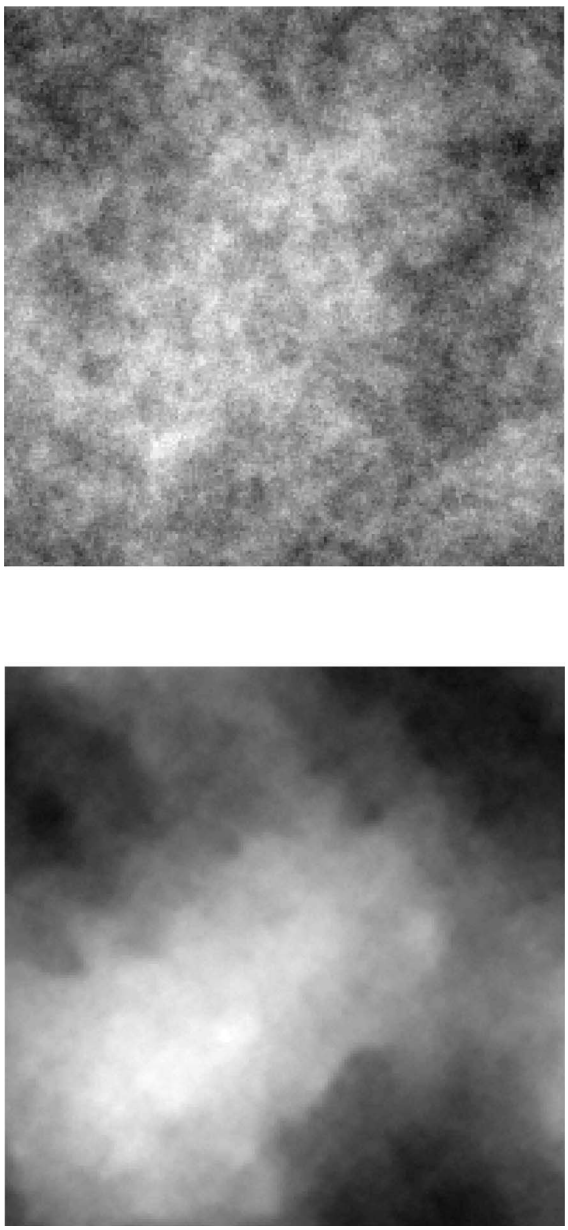

FIG. 4. Two-dimensional FBM distributions of size $n=200\times200$ for $H=0.3$ (top) and $H=0.8$ (bottom), the correlation functions of which are shown in Fig. 3.

such as an oil reservoir. One usually has some data for some of the reservoir's properties, which usually belong to two classes. In one class are the data for *static* properties—those that do not change with time—such as the permeability and porosity that are typically measured or estimated along certain wells in the reservoir. Data for dynamical properties are in the second group, and include the reservoir's rate of oil production and the pressure(s) at the producing well(s). The question then is: Given some (limited) data for the static and dynamical properties of an oil reservoir (or any large-scale porous medium), what is the reservoir's *optimal* model that, (1) honors (preserves) the static data in the areas that have been measured; (2) provides accurate estimates of the same properties in the rest of the reservoir; (3) reproduces the data for the dynamical properties, and (4) provides accurate pre-

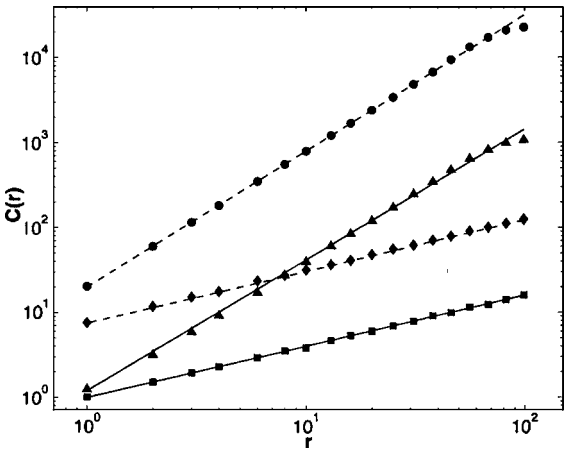

FIG. 5. The correlation functions for 2D anisotropic media of size 200×200. Squares and $\diamond$ show the results for $H=0.3$ in the x and y directions (the x direction is parallel to the lines of this page), while $\triangle$ and $\bigcirc$ indicate those for $H=0.8$ in the same directions, respectively. For $H=0.3$ we set $C_{y1}/C_{x1}=8$, while for $H=0.8$, $C_{y1}/C_{x1}=20$.

dictions for the reservoir's rate of production in the *future*?

To address this question, optimization methods, and in particular simulated annealing (SA) [14], have been utilized [3,15]. One advantage of the SA method is that the static properties do not have to be normally distributed (an assumption made in the classical models of oil reservoirs [2,3]), and may follow any statistical distribution. Moreover, most models of large-scale porous media are constructed based on the assumption that the static properties are spatially *stationary*, whereas the data that follow, for example, the statistics of FBM, are not spatially stationary (only the increments of FBM arrays are stationary). However, the previous works on the development of the optimal model of a large-scale porous medium ignored the long-range correlations in the permeability, porosity, and other static properties. The reason was apparently that it was not clear how to include additional constraints in the "energy" or objective function (that optimization methods minimize) to ensure that the nature of the correlations is preserved. As a result, although the optimal models may honor the existing data, they destroy the correlations in the interwell regions (for which no data are available).

The common methods of generating correlated data described in the Introduction cannot be used in the optimization process, because at each of its steps one changes the values of the properties to be optimized (for example, the permeability, porosity, etc.) for only one block or grid point in the model. It is, therefore, not feasible to generate, at each of the steps, an entirely new array of correlated data, and use only a single value from the large array. In addition, since one must also honor (preserve) the existing data, the array to be generated must be correlated with them, which is clearly not possible to do with the methods described in the Introduction.

This motivated us to develop an optimization method for generating long-range correlations, based on the SA method (although any other suitable optimization method may be used). In our ongoing work [16] we are developing efficient computational algorithms for developing an optimal model of an oil reservoir based on limited data for the porosity and permeability, as well as the pressure(s) at the producing well(s) and seismic data, ensuring that the model preserves the correlations that are indicated by the static data. The method that we describe in this paper is applicable to both isotropic and anisotropic systems.

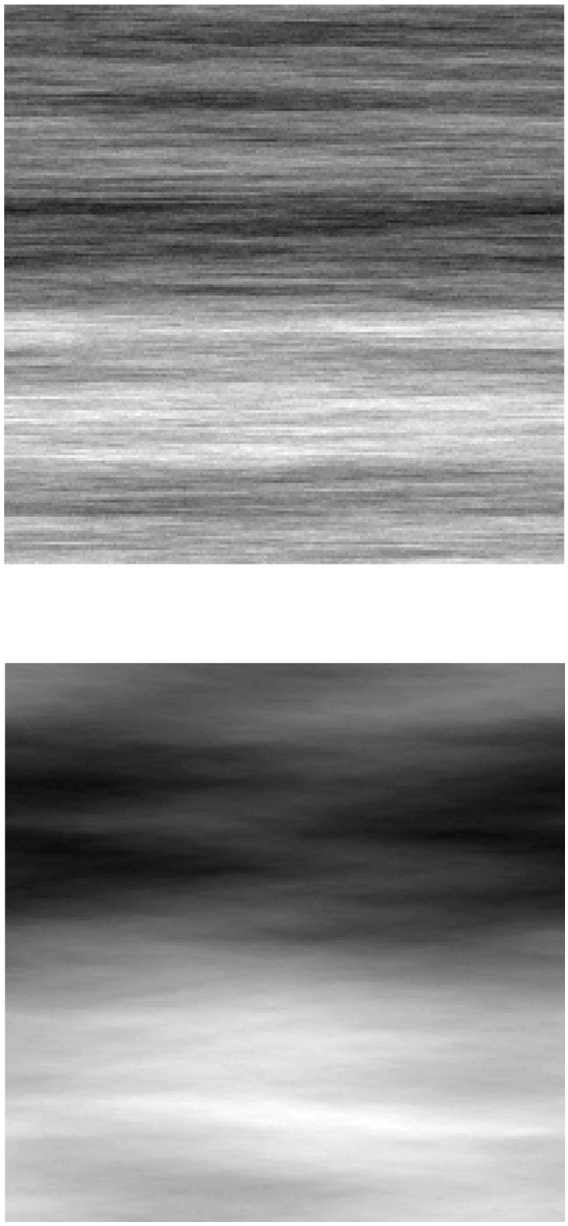

FIG. 6. Two-dimensional anisotropic FBM distributions for $H=0.3$ (top) and $H=0.8$ (bottom), the correlation functions of which are shown in Fig. 5.

A. Isotropic systems

We describe the method for generation of long-range correlations that are characterized by Eq. (1). The method is, however, completely general, so long as the functional form

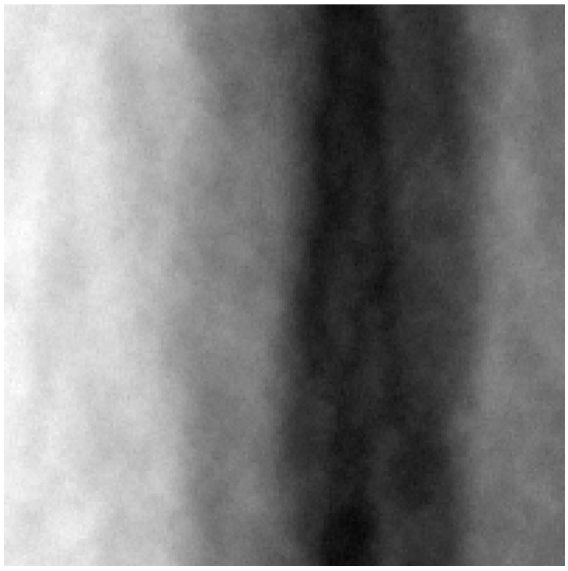

FIG. 7. An example of 2D anisotropic media with $H_x=0.8$, $H_y=0.3$, and $C_{y1}/C_{x1}=1$.

of $C(r)$ is known. The inputs are the Hurst exponent H (obtained from the analysis of the data) and C_1 (which controls the structure of the array; see below). Then, similarly to the SA method [12], we define an objective or energy function E given by

$$E = \sum_r |\log C(r) - 2H \log(r) - \log(C_1)|, \tag{6}$$

which we minimize using the SA algorithm. Clearly, any functional form for the correlation function $C(r)$ may be used in defining E. In addition, note that the algorithm can also be used for generating short-range correlations as well (all one must do is using a function with a cutoff length scale for the correlations), although the generation of such correlations is typically simple enough that using a SA method is not efficient. The following steps are then taken in order to minimize E and generate the correlated array.

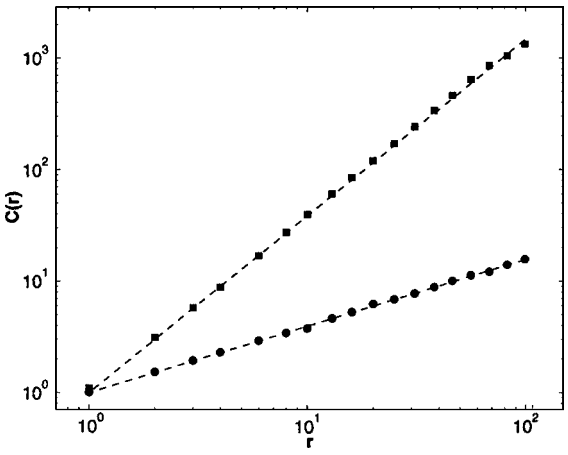

FIG. 8. The directional correlation functions of the 2D anisotropic FBM shown in Fig. 7, for $H_x=0.8$ (squares) and $H_y=0.3$ (○).

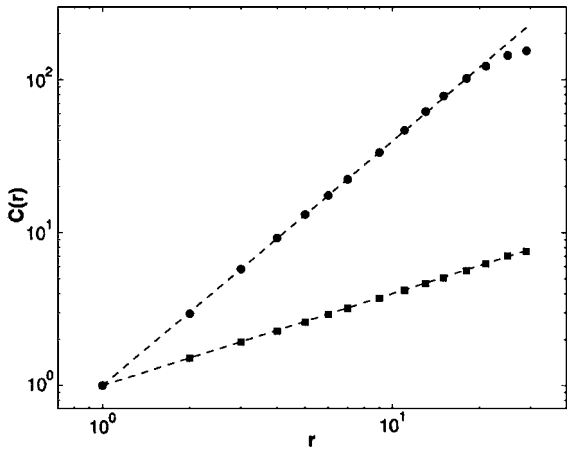

FIG. 9. The correlation functions for 3D FBM arrays of size $n=60\times60\times60$ with $H=0.3$ (squares) and $H=0.8$ (○).

(1) We begin with a Gaussian distribution for the array or lattice (i.e., white noise without correlation). However, any other initial distribution may be used (see below).

(2) The correlation function $C(r)$ is then computed. Note that if there are some actual data distributed in the system that must be honored (preserved), their presence is taken into account when the correlation function $C(r)$ is computed. To speed up the computations, two tricks are used. (i) Except for the first iteration in the optimization process, we compute the *change* in $C(r)$ between successive iterations of the SA, not $C(r)$ itself. This reduces the simulation time very significantly. (ii) $C(r)$ is computed at selected values of $r=r_i$ with $i=1,m,m^2,m^3,\ldots,\frac{1}{2}N$, where N is the array's size, and $m\geqslant1$ is an integer, instead of computing $C(r)$ at r_i with $i=1,2,\ldots,N$, which also reduces the computation time significantly. We have, however, confirmed that the results are the same as those when we compute $C(r)$ at every r_i from $i=1$ to $i=\frac{1}{2}N$.

(3) The initial energy E_{old} is computed, and the initial "temperature" T_0 is set to be $T_0=E_{\text{old}}$.

(4) A site i on the d-dimensional lattice is selected at random, and the value $B(\mathbf{r})$ associated with it is changed. The algorithm for doing so in 1D is to change $B(i)$ to either

$$B_{\text{new}}(i) = B(i+1) + R \tag{7}$$

or

$$B_{\text{new}}(i) = B(i-1) + R, \tag{8}$$

with equal probabilities, where R is a random number selected from a Gaussian distribution with a unit variance, which we found to result in accurate FBM arrays with good computational efficiency. The above algorithm is easily generalized to 2D and 3D. Thus, for example, in 2D, we first select the x or y direction with equal probability. If, for example, the x direction is selected, we change the value $B(i,j)$ attributed to site (i,j) according to $B_{\text{new}}(i,j)=B(i+1,j)+R$ or $B_{\text{new}}(i,j)=B(i-1,j)+R$, with equal probabilities, and similarly for the y direction. Equations (7) and (8) are motivated by the fact that, as mentioned earlier, the successive

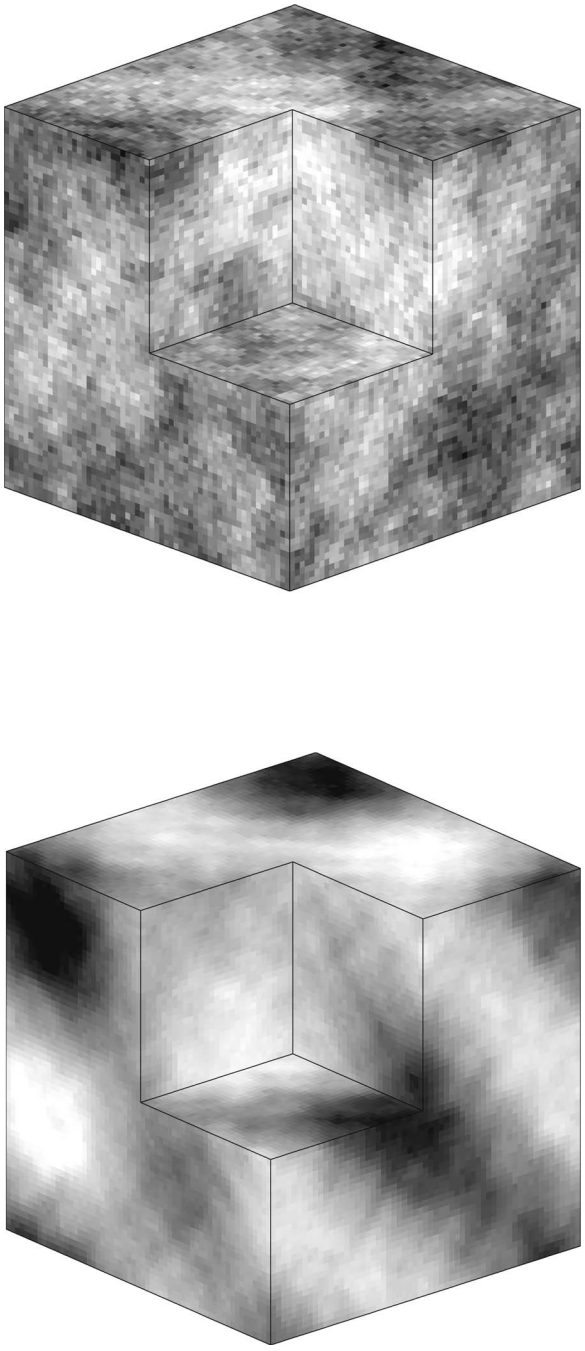

FIG. 10. Three-dimensional FBM distributions of size $n=60\times60\times60$ with $H=0.3$ (top) and $H=0.8$ (bottom), the correlation functions of which are shown in Fig. 9.

increments in a FBM array follow a Gaussian distribution, and selecting R to be a Gaussian distribution ensures that this property is automatically built into the array. However, more generally, one may use other suitable algorithms, instead of Eqs. (7) and (8), or select the random number R from other suitable distributions, depending on the nature of the correlations.

(5) The new energy, E_{new}, and the change in the energy, $\Delta E=E_{\text{new}}-E_{\text{old}}$, are computed. If $E_{\text{new}}<E_{\text{old}}$, the change is accepted and we go back to step (4) and set $E_{\text{old}}=E_{\text{new}}$. If $E_{\text{new}}>E_{\text{old}}$, the change is accepted or rejected using the Metropolis algorithm [i.e., based on a probability proportional to the Boltzmann's factor, $\exp(-\Delta E/T)$]. In any case, we go back to step (4), but keeping track of the number of accepted changes. In addition, we also define and set a maximum number of iterations at each temperature, and a maximum cumulative total change in the energy. When the number of accepted energy changes reach a suitable, *a priori* specified number, or when the maximum allowed changes in the energy is reached or exceeded, step (6) described below is undertaken. Typically, at the initial steps of the SA process (at high temperatures) the accepted changes are achieved before the maximum allowed change is reached or exceeded. At very low temperatures, on the other hand, the maximum allowed changes in the energy are reached before the accepted number of changes reaches its prespecified number, as the number of rejections are large at such temperatures.

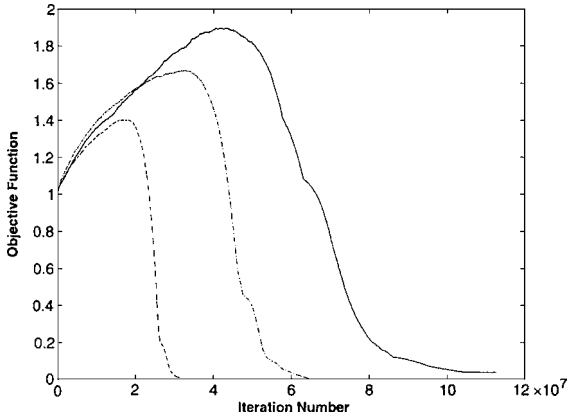

FIG. 11. Variations of the objective function of the optimization process for 3D FBM arrays with $H=0.3$ (dashed curve), $H=0.5$ (dashed-dotted curve), and $H=0.8$ (solid curve).

(6) The temperature is lowered according to the schedule, $T_{\text{new}}=R_T T_{\text{old}}$, where we used $R_T=0.9$ or 0.99.

We also test for convergence to the optimal system. If at any stage ΔE is less than some prespecified value, the iteration is terminated. If not, the temperature is lowered according to the above schedule (after a suitable number of accepted changes is obtained, or if the maximum allowed change is reached or exceeded), and the iteration process continues. The total number of iterations for achieving convergence depends on the system's size and the value of the Hurst exponent H. Convergence is typically reached after the maximum allowed change in the system's energy is achieved or exceeded two or three times.

B. Anisotropic systems

Many natural systems are anisotropic. In particular, in large-scale porous media, such as oil reservoirs, the anisotropy is often caused by stratification, manifested by the existence of many layers that have very different properties. Alternatively, the anisotropy may also be caused by having distinct distributions in the vertical direction and horizontal planes. Such systems are no longer characterized by a single correlation function, but by direction-dependent correlation functions. Hence, to utilize the above algorithm for generat-

ing long-range correlations in an anisotropic medium, we define a series of direction-dependent correlation functions. Consider, for example, the 2D systems. We assume the size of the system to be $N_x \times N_y$, and define suitable correlation functions in the x and y directions, $C_x(r) = C_{x1} r^{2H_x}$ and $C_y(r) = C_{y1} r^{2H_y}$. The objective function to be minimized is then given by

$$E = \sum_{j=1}^{N_y} \sum_{i=1}^{N_x/2} |\log C_x(r_i, r_j) - 2H_x \log(r_i) - \log(C_{x1})| + \sum_{i=1}^{N_x} \sum_{j=1}^{N_y/2} |\log C_y(r_i, r_j) - 2H_y \log(r_j) - \log(C_{y1})|. \quad (9)$$

Generalization of Eq. (9) to 3D systems is straightforward.

Note that allowing for distinct, direction-dependent values of the Hurst exponent is motivated by the fact that field scale data often indicate distinct Hurst exponents for the vertical direction and in the planes perpendicular to it. Physically, this is understandable as the strata are roughly parallel to each other and to the ground surface. Since the strata have contrasting properties, one expects to have negative correlations in the vertical direction, characterized by $H_z < 0.5$, while in the planes of the strata (within the strata) one expects to have positive correlations with $H_x = H_y > 0.5$. Although the contrasting properties of the strata can also be associated with a stochastic fluctuation term with a large variance, extensive field data for many oil reservoirs do confirm [3] the expectation of having $H < 0.5$ in the vertical direction and $H > 0.5$ within the strata more or less parallel to the ground surface. Note also that *none* of the existing methods can generate long-range correlations with distinct, direction-dependent Hurst exponents.

During the SA iteration, we utilize the following algorithm in order to change the value $B(i,j)$ attributed to site (i,j) on a 2D lattice, which is a generalization to anisotropic systems of the algorithm described by Eqs. (7) and (8):

$$B_{\text{new}}(i,j) = B(i+1,j) + R \quad (10)$$

or

$$B_{\text{new}}(i,j) = B(i-1,j) + R \quad (11)$$

with equal probabilities, and

$$B_{\text{new}}(i,j) = B(i,j+1) + \left(\frac{C_{y1}}{C_{x1}}\right) R \quad (12)$$

or

$$B_{\text{new}}(i,j) = B(i,j-1) + \left(\frac{C_{y1}}{C_{x1}}\right) R, \quad (13)$$

again with equal probabilities, where R is a random number distributed according to a Gaussian distribution. The generalization to 3D systems is straightforward. The rest of the optimization algorithm is the same as that for the isotropic systems described above.

III. RESULTS AND DISCUSSION

We now present the results and discuss the accuracy and efficiency of the method.

A. Accuracy of the method

Figure 1, mentioned in the Introduction, presents examples of 1D FBM arrays generated by the optimization method described above. The corresponding correlation functions $C(r)$ are shown in Fig. 2, where they presented as the logarithmic plot of $C(r)$. In this and the following figures the distance r is measured in units of the distance between two nearest-neighbor sites in the lattice. The straight lines shown in Fig. 2 indicate that the correct correlation function has been generated by the SA method. Note that, for $H > 0.5$, the correlation function at the highest value of r is slightly bent. This is a finite-size effect, which is also seen for higher-dimensional FBM arrays described below. At the same time, we note that, over large ranges of r and for certain values of the parameter γ of Eq. (3), the correlation functions that are generated by the method of Makse *et al.* [8] are very irregular, even in log-log plots (see their Fig. 1).

Figure 3 shows the correlation functions for 2D isotropic FBM arrays and two values of the Hurst exponent H. The size of the array is 200×200 and, once again, the correlation function follows very precisely the expected behavior indicated by Eq. (1). The corresponding samples of 2D FBM arrays are presented in Fig. 4, where the darkest and lightest regions indicate, respectively, the highest and lowest values.

Next, we consider 2D anisotropic systems, with the anisotropy generated by stratification, or by having distinct distributions in different directions. Figure 5 presents the direction-dependent correlation functions $C_x(\mathbf{r})$ and $C_y(\mathbf{r})$ for two values of the Hurst exponent $H = H_x = H_y$. Once again, all the 1D correlation functions follow precisely the expected behavior. The corresponding 2D samples of the FBM arrays are shown in Fig. 6. The orientation and the number of layers can be varied by changing the ratio C_{y1}/C_{x1}. As pointed out above, one may also have anisotropic media that are characterized by distinct values of H_x and H_y (in 3D, $H_x = H_y \neq H_z$). An example is shown in Fig. 7, with its corresponding correlation functions shown in Fig. 8.

The accuracy of the method in generating 3D arrays is similar to those for 1D and 2D arrays. Figure 9 presents the correlation function $C(r)$ for a $60 \times 60 \times 60$ lattice and two values of the Hurst exponent H which demonstrates, once again, the accuracy of the method in generating 3D correlated arrays with a correlation function that follows Eq. (1). The corresponding 3D FBM samples are shown in Fig. 10.

B. Efficiency of the method

Figure 11 presents the behavior of the objective or energy function E in isotropic 3D systems, exhibiting the trends discussed above. For all values of H, the objective function first reaches a maximum, and then decreases. The trends will not change if the initial distribution that we begin the SA algorithm with is changed to a uniform or some other type of distribution function, since one complete sweep of the sys-

TABLE I. Comparison of the computation time (in CPU seconds) of four methods of generating a 200×200 FBM array with the Hurst exponent $H=0.3$, which are fast Fourier transformation (FFT), successive random addition (SRA), the Weierstrass-Mandelbrot (WM) function, and simulated annealing (SA) suggested in the present paper.

FFT	SRA	WM	SA
0.3	0.6	0.6	8

tem completely changes the initial distribution. The trends do not change for anisotropic media either. Completely similar trends are obtained for 1D and 2D media and, therefore, are not shown.

In general, our experience is that Hurst exponents $H<0.5$ require about one order of magnitude fewer iterations of the SA algorithm than those for $H>0.5$, in order to converge to the desired correlation function. We believe, based on our experience, that the reason might be due to the fact that $H<0.5$ generates negative or anticorrelations, implying that a high (low) value at any point of the array is likely to be followed by a low (high) value. The magnitude of such changes does, of course, depend on the magnitude of the Gaussian random number R. But, in any case, a medium with $H<0.5$ is, in some sense, more disordered than one with $H>0.5$. Therefore, since for each iteration of the SA algorithm, we change the values of the array according to Eqs. (7), (8), and (10)–(13) (and their analogs in higher dimensions) using Gaussian numbers R, it might, in some sense, be easier to generate negative correlations as R is selected at random from a Gaussian distribution. At the same, we should keep in mind that after one complete sweep of the initial guess, its structure is destroyed and becomes random. The new random distribution corresponds to one with $H=-d/3$ [see Eq. (2)]. It is clearly easier (it requires fewer iterations) to construct a FBM distribution with a smaller H closer to a random distribution. While our argument might be plausible, one can also argue that, in general, one expects the rate of convergence to depend on the magnitude of the random variable R in Eqs. (7), (8), and (10)–(13). At the same time, negative or positive correlations depend on the compared signs of successive increments, and are properties that characterize the correlations of the random jumps for both $H<0.5$ and $H>0.5$. Therefore the randomness of the increments should not be more particularly associated with positive correlations than to negative ones.

The method presented in this paper is slower than those based on the spectral density by about one order of magnitude. For example, Table I compares the required CPU times for generating a 200×200 FBM array, using the three methods described in the Introduction, as well as the method proposed in this paper based on simulated annealing. All the times are for a Pentium-4 desktop (with a 2.8 GHz CPU). However, as discussed above, the method proposed in the present paper has a few distinct advantages over the previous techniques of generating long-range correlations.

(1) The method is designed precisely for some important physical problems involving optimization, for which other methods of generating long-range correlations (see the Introduction) *cannot* be used. For example, none of the previous methods can generate long-range correlations, and *at the same time* honor (preserve) experimental data for the system under study.

(2) The method is, on its own, still efficient in terms of the computation time that it requires and, therefore, can be used for generation of long-range correlations in systems with hundreds of thousands of points or more.

(3) In practice, the algorithm proposed here is incorporated into a larger optimization problem involving many parameters (data) and constraints imposed on the system. In that case, the computation time for generating the long-range correlations by the method proposed in this paper is a very small fraction of the total computation time [16].

IV. SUMMARY

Formulating generation of long-range correlations in large systems as an optimization problem, we developed an algorithm based on simulated annealing that generates the desired correlations, but also honors experimental data that are to be incorporated in the model. The method is completely general and applicable to d-dimensional isotropic as well as anisotropic systems. In addition, it is applicable to any type of correlation function for the data. The method is also efficient and, therefore, can be used for generating correlations in large systems.

ACKNOWLEDGMENTS

The work of H.H. was supported in part by the NIOC. We would like to thank S.M. Vaez Allaei for very useful discussions.

[1] P. M. Adler and J.-F. Thovert, *Fractures and Fracture Networks* (Kluwer, Dordrecht, 1999).

[2] H. H. Hardy and R. A. Beier, *Fractals in Reservoir Engineering* (World Scientific, Singapore, 1994).

[3] M. Sahimi, Rev. Mod. Phys. **65**, 1393 (1993); *Flow and Transport in Porous Media and Fractured Rock*, 2nd ed. (VCH, Weinheim, Germany, 2006).

[4] M. Sahimi and S. E. Tajer, Phys. Rev. E **71**, 046301 (2005).

[5] R. Friedrich and J. Peinke, Phys. Rev. Lett. **78**, 863 (1997); J. Davoudi and M. R. Tabar, *ibid.* **82**, 1680 (1999); C. Renner, J. Peinke, and R. Friedrich, J. Fluid Mech. **433**, 383 (2001).

[6] J. B. Bassingthwaighte, L. S. Liebovitch, and B. J. West, *Fractal Physiology* (Oxford University Press, New York, 1994); C.-K. Peng, J. Mietus, J. M. Hausdorff, S. Havlin, H. E. Stanley, and A. L. Goldberger, Phys. Rev. Lett. **70**, 1343 (1993); J. M. Hausdorff, P. L. Purdon, C.-K. Peng, Z. Ladin, J. Y. Wei,

and A. L. Goldberger, J. Appl. Physiol. **80**, 1448 (1996); P. Bernaola-Galvan, P. Ch. Ivanov, L. A. Nunes Amaral, and H. E. Stanley, Phys. Rev. Lett. **87**, 168105 (2001).

[7] See, however, F. Ghasemi, J. Peinke, M. Sahimi, and M. R. Rahimi Tabar, Eur. Phys. J. B **47**, 411 (2005); F. Ghasemi, J. Peinke, M. R. Rahimi Tabar, and M. Sahimi, Int. J. Mod. Phys. C **17**, 1 (2006); M. R. Rahimi Tabar *et al.*, Comput. Sci. Eng. **8**, 54 (2006), for a different view point.

[8] H. A. Makse, S. Havlin, M. Schwartz, and H. E. Stanley, Phys. Rev. E **53**, 5445 (1996).

[9] A. R. Mehrabi, H. Rassamdana, and M. Sahimi, Phys. Rev. E **56**, 712 (1997).

[10] N.-N. Pang, Y.-K. Yu, and T. Halpin-Healy, Phys. Rev. E **52**, 3224 (1995).

[11] R. F. Voss, in *Fundamental Algorithms for Computer Graphics*, edited by R. A. Earnshaw, *NATO ASI Series, Vol. 17* (Springer-Verlag, Heidelberg, 1985), p. 805; S. Lu, F. J. Molz, and H.-H. Liu, Comput. Geosci. **29**, 15 (2003).

[12] M. Ausloos and D. H. Berman, Proc. R. Soc. London, Ser. A **400**, 331 (1985); W. Yan and K. Komvopoulos, J. Appl. Phys. **84**, 3617 (1998).

[13] J. L. Jensen, L. W. Lake, P. W. M. Corbett, and D. J. Goggin, *Statistics for Petroleum Engineers and Geoscientists*, 2nd ed. (Elsevier, Amsterdam, 2000).

[14] S. Kirkpatrick, C. D. Gellat Jr., and M. P. Vecchi, Science **220**, 671 (1983).

[15] See, for example, M. Sen and P. L. Stoffa, *Global Optimization Methods in Geophysical Inversion* (Elsevier, Amsterdam, 1995); F. D. Day-Lewis, P. A. Hsieh, and S. M. Gorelick, Water Resour. Res. **36**, 17071721 (2000); C. E. Romero and J. N. Carter, J. Pet. Sci. Eng. **31**, 113 (2001).

[16] H. Hamzehpour and M. Sahimi (unpublished).